Imidazolyl-Tailed Tetrakis(pivalamidophenyl)porphyrinatocobalt (II): An Efficient Oxygen Adsorbent Molecule

Hiroyuki Nishide,* Ayako Suzuki, and Eishun Tsuchida*,#

Department of Polymer Chemistry, Waseda University, Tokyo 169

(Received February 24, 1997)

A *meso*-tetrakis($\alpha,\alpha,\alpha,\alpha$-*o*-pivalamidophenyl)porphyrinatocobalt(II) derivative bearing covalently-bound imidazole (Scheme 1, CoPim) was synthesized. Oxygen-binding to CoPim was rapid and reversible. The CoPim in the solid state chemically adsorbed oxygen (20 ml O_2/g CoPim), which was ca. 40-times greater than the physical adsorption amount. The oxygen-binding lifetime of CoPim was longer than that for the corresponding porphyrinatocobalt(II) with an externally added imidazole. The efficiency of CoPim as an oxygen carrier was demonstrated by oxygen-enrichment from air using a pressure-swing adsorption experiment.

Porphyrinatometal derivatives were exhaustively synthesized as oxygen-carrying molecules for the decade before and after 1980, and their oxygen-binding kinetics and equilibrium were studied in comparison with those of hemoglobin and myoglobin.[1)] A typical example is the iron or cobalt complex of *meso*-tetrakis($\alpha,\alpha,\alpha,\alpha$-*o*-pivalamidophenyl)porphyrin of Collman (Scheme 1, CoP).[1a,2)] This porphyrin has a steric "picket fence" constructed with four pivalamido groups on one side of the plane, leaving the other side unencumbered. An externally added imidazole ligand is allowed to combine with the unhindered side of the porphyrinatometal, with the other side remaining as a cavity for oxygen-binding. Here, the imidazole ligand coordinates to the fifth site of the central metal ion of porphyrin and improves the affinity with the oxygen molecule, which coordinates to the sixth site of the metal ion. Moreover, the picket fence inhibits an irreversible side-reaction via the μ-dioxodimer formation.

Air separation is industrially performed using oxygen-permselective polymer membranes and nitrogen adsorbents such as zeolites, besides cryogenical distillation of air, and new materials, including porphyrinatometals, for such membranes and adsorbents are still an important research subject.[3)] New porphyrinatoiron derivatives as oxygen carriers are also still being synthesized for their application to artificial red cells or blood substitutes.[4)] However, these porphyrinatometals and their oxygen-binding property have been studied in aqueous or organic solutions and by dispersing in polymer matrices; little is known about the porphyrinatometals themselves as oxygen adsorbents in the solid state.

This paper describes a porphyrinatocobalt derivative, which in the solid powder state rapidly and reversibly binds oxygen and acts as an oxygen adsorbent without any additives, such as an imidazole. To maintain the five-coordinated porphyrinatocobalt structure represented in CoP of Scheme 1 with the oxygen-binding affinity, an excess amount of the imidazole has to be added to the porphyrinatocobalt. We have already synthesized and reported on the porphyrin bearing a 2-methylimidazol-1-ylalkyl group with a covalent bond.[5,6)] In this study, this porphyrin was converted to its cobalt(II) derivative with a covalently-bound imidazol-1-ylalkyl group; 2-[8-(Imidazol-1-yloctanoyloxymethyl)]-*meso*-tetrakis($\alpha,\alpha,\alpha,\alpha$-*o*-pivalamidophenyl)porphyrinatocobalt(II) (Scheme 1, abbreviation: CoPim), because cobalt(II)–porphyrins possess a greater stability against irreversible oxidation of the central metal ion, here the oxidation of Co(II) to Co(III), compared with the corresponding porphyrinatoirons(II). Cobalt Schiff's base chelates, such as *N*,*N*′-disalicylideneethylenediaminocobalt-(II), have been well studied to form the μ-dioxo-type oxygen adduct represented by Co–O_2–Co.[8)] However, these cobalt chelates lack rapid oxygen-releasing and/or reversibility in the oxygen-binding. The imidazolyl-tailed porphyrinatocobalt can be expected to be the most compact oxygen-selective adsorbent, which reversibly reacts with oxygen in response to the atmospheric oxygen concentration.

Experimental

2-[8-(Imidazol-1-yloctanoyloxymethyl)]-*meso*-tetrakis($\alpha,\alpha,\alpha,\alpha$-*o*-pivalamidophenyl)porphyrin. This title compound was synthesized according to our previous paper[6)] by reacting *meso*-tetrakis($\alpha,\alpha,\alpha,\alpha$-*o*-pivalamidophenyl)porphyrinatocopper(II) with Vilsmeier reagent in order to introduce the formyl group at the β-pyrrolic position, removing copper(II) from the porphyrin, reducing the aldehyde to the alcohol, and binding 8-(imidazol-1-yl)octanoic acid to the porphyrin by a dicyclohexylcarbodiimide-coupling.

2-[8-(Imidazol-1-yloctanoyloxymethyl)]-*meso*-tetrakis($\alpha,\alpha,\alpha,\alpha$-*o*-pivalamidophenyl)porphyrinatocobalt(II) (CoPim). A chloroform solution (100 ml) of 2-[8-(imidazolyl-1-yloctanoyloxymethyl)]- *meso*- tetrakis($\alpha,\alpha,\alpha,\alpha$- *o*- pivalamidophenyl)porphyrin (0.78 g, 0.63 mmol) and triethylamine (1 ml, 7.4 mmol) was added

CREST investigator, JST.

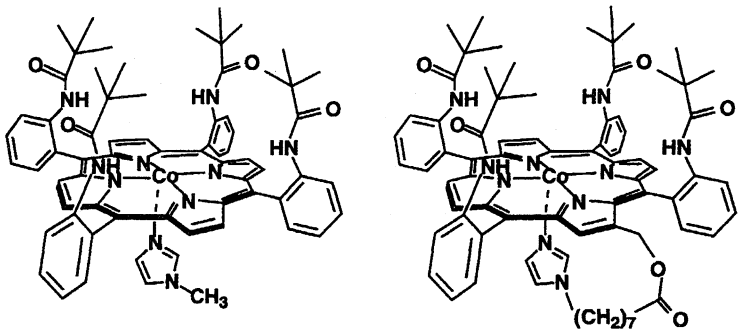

CoP-Im **CoPim**

Scheme 1.

dropwise to a methanol solution (50 ml) of cobalt(II) acetate tetrahydrate (6.3 g, 25 mmol), and mixture was refluxed for 1 d. The mixture was then brought to dryness, the residue was again dissolved in chloroform, insoluble unreacted cobalt acetate was filtered off, and the filtrate was evaporated to dryness. The residue was again dissolved with chloroform and filtered through an aluminum column. The resulting solution was chromatographed on a silica-gel flash column using chloroform/methanol (15/1 v/v) as the eluent ($R_f = 0.24$). The eluate was collected and evaporated to dryness. The residue was then dried at room temperature for 1 d in vacuo to give a purple product. Yield: 0.7 g, 85%. MS *m/z* (FAB) 1289 (M^+); UV/vis λ_{max} (chloroform) 533 and 424 nm.

As a control, *meso*-tetrakis($\alpha,\alpha,\alpha,\alpha$-*o*-pivalaminophenyl)-porphyrin was prepared as described in the literature.[7] *N*-Methylimidazole (Im) was used as the ligand of CoP; CoP–Im was prepared by a chloroform solution of CoP and Im (molar [Im]/[CoP] = 100) under a nitrogen atmosphere and dried in vacuo for 2 d to give the CoP–Im and to remove any excess Im.

Spectroscopic Measurements. ^{1}H NMR spectra were recorded on a JEOL GSX-270 spectrometer. FAB mass spectra were measured with a JEOL DX-303 spectrometer. ESR spectra were taken on a JEOL JES-2XG ESR spectrometer with 100-kHz field modulation.

Oxygen-binding to CoPim was also measured by a spectral change in its visible absorption using a UV spectrophotometer (Shimadzu Model UV-2100). For measuring the CoPim in the solid state, the powder of CoPim was deposited on the wall of a Thunberg-type cell by slowly evaporating the CoPim toluene solution, which was sufficiently transparent to measure the visible absorption. The oxygen-binding kinetics were studied with a pulsed laser-flash spectrophotometer (Unisoku TSP-601). Monitoring wave-lengths of 410 and 430 nm were selected, which agreed with the maxima of the deoxy- and oxy-CoPim, respectively. The oxygen-binding and -dissociation rate constants were calculated by a pseudo-first-order kinetics analysis in the time course at these absorbances. The oxygen-binding equilibrium and kinetic constants were determined to two significant figures.

Adsorption Measurements. The adsorbed amounts of oxygen and nitrogen to the powder samples were measured based on the pressure decrease with a Baratron absolute pressure gauge (MKS Instr. KA-102) under the condition of constant volume. The apparatus consisted of a vacuum line mounted in a thermocontrolled air bath.

The pressure-swing adsorption experiment was examined by assembling the apparatus (Scheme 2). The CoPim powder (6.2 g) was packed in the chamber (20 ml) of the apparatus. The electromagnetic valves (V_a and V_b) were opened to the exhausted line, and the dried air was blown into the chamber. V_a was then closed and V_b was opened to the pump line to decrease the pressure in the chamber (70—100 mmHg, 1 mmHg = 133.322 Pa). The volume of gas flowed out; the maximum and averaged oxygen concentrations which accumulated in the tank were measured. V_a and V_b were controlled by the timer, and the pressure in the chamber was also measured.

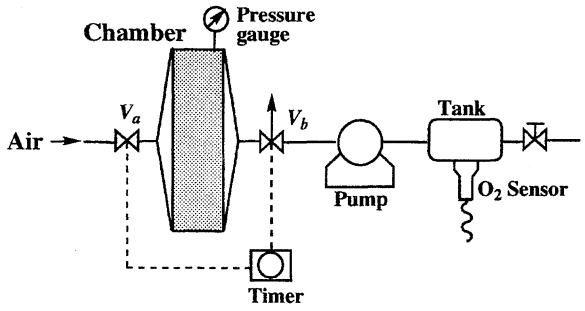

Scheme 2.

Results and Discussion

Oxygen-Binding Reaction to the CoPim. Intramolecular coordination of the tailed-imidazole to porphyrinatocobalt in toluene was first recognized by ESR spectoroscopy. In the absence of oxygen, the ESR signal gave an eight-line hyperfine splitting spectrum with the following parameters: $g_{\|} = 2.05$, $g_{\perp} = 2.33$, and $A_{\|}^{Co} = 78$ G. These agreed with the parameters previously reported for the same CoP coordinate with externally added *N*-methylimidazole (CoP–Im) ($g_{\|} = 2.04$, $g_{\perp} = 2.31$, and $A_{\|}^{Co} = 78$ G[7]). The hyperfine splitting and the parameters were attributed to the nitrogen on the Co's fifth coordination site, and indicated that the tailed-imidazole coordinated to the Co and that CoPim took a five-coordinated structure maintaining its sixth coordination site vacant for oxygen-binding. The visible absorption spectrum of the CoPim toluene solution gave a strong Q-band peak with $\lambda_{max} = 533$ nm assigned to a five-coordinated porphyrinatocobalt, without any shoulder absorptions ascribed to a four- or six-coordinated porphyrinatocobalt.

A disproportionate coordination of imidazolyl-tailed porphyrinatometals has sometimes been reported: e.g., two imidazolyl-tailed protoporphyrinatoirons do not form two

intramolecular five-coordinated porphyrinatoiron, but one intermolecular six-coordinated porphyrinatoiron and one four-coordinated porphyrinatoiron are formed under the conditions of its high concentration solution and at low temperature.[11] However, the visible absorption spectra of the toluene solution of CoPim gave only a simple absorption peak at 533 nm, ascribed to the five-coordinated porphyrinatocobalt, even in a high concentration of several mM (1 M=1 mol dm^{-3}) and even at −15 °C. This preferential formation of the intramolecular five-coordinated structure for CoPim is considered to be caused by both the picket-fence structure on one side of the porphyrin plane and a favorable property of porphyrinatocobalt for five-coordination.

The visible absorption spectrum of the deoxy CoPim (λ_{max}=533 nm) was changed to the spectrum with λ_{max}=548 nm assigned to the oxygen adduct (oxy) of the CoPim immediately after exposure to oxygen. The oxy-deoxy spectral change was rapid and reversible in response to the partial oxygen pressure of the atmosphere, with isosbestic points at 480, 538, and 669 nm. After introducing air to the CoPim, the ESR gave a slightly rhombic distorted hyperfine splitted ESR spectrum with $g_\perp$=2.03 and $A_{\parallel}^{Co}$=17 G ($g_\perp$=2.01, $A_{\parallel}^{Co}$ ca. 20 G in CoP–Im). This spectrum revealed the formation of an oxygen adduct of CoPim (O_2/Co=1/1). These ESR and visible absorption spectra indicated appropriate coordination of the tailed-imidazole of CoPim to Co and an oxygen adduct formation the same as that for CoP–Im.

The oxygen-binding affinity (p_{50}: the oxygen partial pressure at 50% of oxygen-binding) or the equilibrium constant in the oxygen-binding reaction (Eq. 1) of CoPim was determined from the oxygen-binding equilibrium curves, which were drawn based on the visible spectral change of CoPim from the oxygen partial pressure (p_{O_2}) of 0 to p_{O_2} of 76 cmHg (Fig. 1). The curves obey Langmuir's isotherm, which gave the p_{50} values listed in Table 1. The oxygen-binding affinity or p_{50} of CoPim was comparable with that of CoP–Im

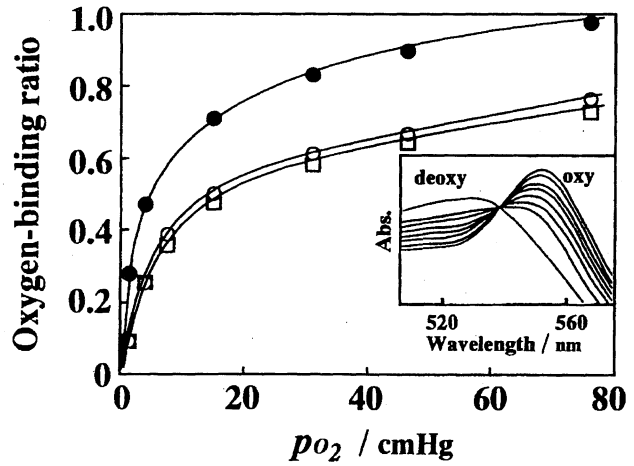

Fig. 1. Oxygen-binding equilibrium curves of the porphyrinatocobalts at 25 °C. (●): CoPim in the solid state, (○): CoPim in 10 mM toluene solution, (□): CoP–Im in 10 mM toluene solution. p_{O_2}: partial oxygen pressure. Inset: Visible absorption spectral change at p_{O_2} = 0—78 cmHg.

Table 1. Oxygen-Binding Affinity, Enthalpy and Entropy Changes, and Rate Constants of the Porphyrinatocobalts (25 °C)

Porphyrin	State	p_{50}	ΔH	ΔS	$10^{-8}k_{on}$	$10^{-5}k_{off}$
		cmHg	kcal mol^{-1}	eu	M^{-1} s^{-1}	s^{-1}
CoPim	Toluene	13.2	−12	−39	7.5	5.4
	Solid	5.8	−13	−38	—	—
CoP–Im	Toluene	14.0	−12	−38	6.8	4.4
	Solid	6.9	−13	−38	—	—

both in the toluene solution and in the solid powder state. The affinities of CoPim and CoP–Im in the solid state were greater (p_{50} were smaller) than those in the toluene solution. This difference could be reduced by the oxygen solubility in toluene, and the infinite affinity of the porphyrinatocobalts was not affected by their solution and solid state.

$$O_2 + CoPim \underset{k_{off}}{\overset{k_{on}}{\rightleftarrows}} O_2\text{–}CoPim \quad (1)$$

Enthalpy and entropy changes (ΔH and ΔS) for the oxygen-binding were determined from the temperature dependence of p_{50}, and are also given in Table 1. The ΔH and ΔS values of CoPim were almost the same as those of CoP–Im.

The photodissociation and recombination of bound oxygen to and from CoPim in the toluene solution were observed by laser flash photolysis. The oxygen-binding and -dissociation rate constants (k_{on} and k_{off} in Eq. 1) were estimated using pseudo-first-order kinetics on the spectral time courses in the oxygen recombination, and are also given in Table 1. The k_{on} and k_{off} values of CoPim were also comparable with those of CoP–Im, which resulted in the same steric structure in the oxygen-binding cavity.

The apparent oxygen-binding and -dissociation rate constants (k'_{on} and k'_{off}, respectively) to and from CoPim in the solid powder state were also estimated by analyzing the time courses of oxygen ad- and desorption with visible absorption spectroscopy (Fig. 2). They were analyzed based on the pseudo-first-order kinetics of the Langmuir isotherm, and are listed in Table 2. k'_{on} and k'_{off} give the apparent oxygen-binding equilibrium constant (K') in Table 2, which is almost coincident with the reverse of p_{50} determined from the equilibrium curve and given in Table 1. This supported the validity of the kinetic analysis. The k'_{on} and k'_{off} values of CoPim were almost the same as those of CoP–Im, and CoPim in the solid powder state maintained its rapid and reversible oxygen-binding capability, as did CoP–Im.

Lifetime of CoPim as an Oxygen Carrier. The crucial characteristic of porphyrinatocobalts as oxygen carriers is their lifetime of the oxygen-binding function. The half-lives (τ) of CoPim in the toluene solution and the solid powder state were observed upon exposure of ambient laboratory air at room temperature by measuring the irreversible oxidation of Co(II)Pim to Co(III)Pim or the increase in the visible absorption ascribed to the Co(III)Pim without an oxygen-binding capability at λ_{max}=555 nm with the passage of time (Table 3). The τ of CoPim in the toluene solution was shorter

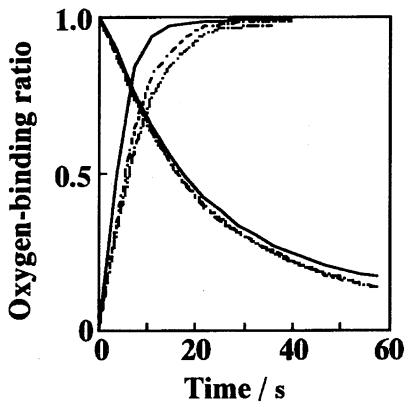

Fig. 2. Time course of the oxygen adsorption and desorption (relative change) to and from CoPim in the solid powder state at 25 °C. Adsorption from nitrogen atmosphere under the supplement of various oxygen/nitrogen mixed gases, p_{O_2} = (- - -): 0.54, (– – –): 15.1, (——): 76 cmHg. Desorption under the supplement of the mixed gases, p_{O_2} = (- - -): 0, (– – –): 61, (——): 75 cmHg. Monitoring wavelength 548 nm assigned to oxy.

Table 2. Apparent Oxygen-Binding and -Dissociation Rate Constants of the Porphyrinatocobalts in Solid State (25 °C)

Porphyrin	$10^3\ k'_{on}$ / $cmHg^{-1}\ s^{-1}$	$10^2\ k'_{off}$ / s^{-1}	$10\ K'$ / $cmHg^{-1}$
CoPim	9.5	7.0	1.4
CoP–Im	8.6	7.2	1.2

Table 3. Half-Life (τ) of the Porphyrinatocobalts upon the Exposure of Laboratory Air at Room Temperature

Porphyrin	τ/h	
	Toluene	Solid
CoPim	13±2	41±5
CoP–Im	24±2	22±6

than the τ of CoP–Im, probably because of a slight distortion in the coordination of the tailed-imidazole. However, CoPim in the solid state was more stable than CoPim in the solution and than CoP–Im in the solid state. The powder state CoPim acted as a long-life oxygen carrier at ambient atmosphere.

The irreversible oxidation process of porphyrinatometals during their oxygen-binding reaction has been summarized in the following three pathways: (i) μ-dioxo dimerization to form μ-oxo Co(III)P dimer (Eq. 2), (ii) proton-driven oxidation caused by the attack of a water or protic molecule (Eq. 3), and (iii) intramolecular oxidation via moment base-off (Eq. 4), by using the example of CoP–Im.

$$\text{Im–CoP–O}_2 + \text{CoP–Im} \rightleftarrows \text{Im–CoP–O}_2\text{–CoP–Im} \longrightarrow \text{Co(III)P–O}^{2-}\text{–Co(III)P} \quad (2)$$

$$\text{Im–CoP–O}_2 + \text{H}^+(\text{H}_2\text{O}) \longrightarrow \text{Im–Co(III)P–OH}^- + \text{HO}_2^{-*} \quad (3)$$

$$\text{Im–CoP–O}_2 \rightleftarrows \text{Im} + \text{Co(II)P–O}_2 \longrightarrow \text{Im–Co(III)P} + \text{O}_2^{-*} \quad (4)$$

The lifetime of the oxygen adduct of CoPim in toluene was decreased with the addition of a small amount of methanol (1 mM—5 M). The τ was represented as

$$1/\tau = 0.0071\,[\text{CH}_3\text{OH}]^{1.0} + 0.018, \quad (5)$$

which indicated the proton-driven process for the irreversible oxidation of CoPim. The lifetime of CoPim in the solid powder state was reduced by almost half upon exposure to air with 46% relative humidity (τ=20 h). Especially, τ for the CoP–Im powder was decreased ca. one-fifth under humid air. CoP–Im was hygroscopic because it was contaminated with externally added Im during its preparation, and the uptaken water probably accelerated the proton-driven oxidation for the CoP–Im powder. Additionally, static bonding of the imidazole ligand with CoP in the solid state retards the irreversible oxidation process of Eq. 4, which is considered to be further suppressed for CoPim based on its tailed-imidazole or intramolecular covalently bonded structure.

Oxygen Adsorption Ability of the CoPim Powder. The adsorption isotherm of oxygen for CoPim in the solid powder state is shown in Fig. 3. The isotherm obeyed a Langmuir one. The oxygen-binding equilibrium constant determined by the Langmuir isotherm was K=0.13 $cmHg^{-1}$, which agreed with the K and p_{50} values spectroscopically estimated as previously mentioned. The saturated oxygen adsorption amount was 24 ml O_2/g CoPim (which corresponded to 72 mol % of the fed CoPim in the measurement). The oxygen adsorption amount at p_{O_2}=50 cmHg (20 ml O_2/g CoPim) was ca. 40-times greater than the physical adsorption amount of nitrogen. The CoPim powder acted as an efficient oxygen adsorbent.

The pressure swing adsorption (PSA) method was applied to examine the capability of the CoPim powder as an oxygen adsorbent. PSA is now industrially performed to separate air

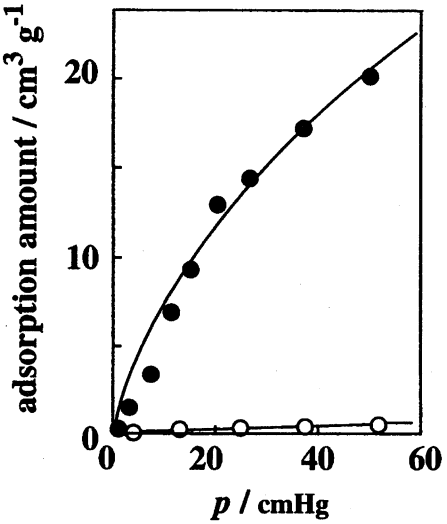

Fig. 3. Adsorption isotherms of oxygen (●) and nitrogen (○) for CoPim in the solid powder state at 30 °C.

Table 4. Oxygen-Enrichment with the CoPim Adsorbent by Pressure Swing Adsorption Method (25 °C)

Interval	O_2 concn in product	
s	Max %	Ave %
10	33	26
30	45	33
60	52	38

to produce 30% oxygen–air using zeolites, which selectively adsorb nitrogen from air. However, there remain the following problems for the PSA using the nitrogen adsorbent: (i) A multi-column (or -chamber) apparatus is essential because nitrogen desorption or regeneration of the adsorbent consumes time in comparison with the air supplied to the column or chamber. (ii) The adsorption capacity of zeolites is small. (iii) Their nitrogen/oxygen selectivity is less than 5. An oxygen adsorbent is to satisfy the following conditions for the PSA method: (i) adsorption capacity and oxygen selectivity from air, (ii) high adsorption at air pressure (p_{O_2}=15 cmHg) and desorbing more than 30% of the adsorbed oxygen at a reduced pressure of 7—10 cmHg with a small pump (p_{O_2}=1.5—2 cmHg), and (iii) high desorption rate to increase the cycle of ad- and desorption per time.

Performance examples of the PSA experiment are listed in Table 4. Oxygen-enriched air (30—40% oxygen concentration) was continuously produced with the compact PSA device using the CoPim powder which rapidly and selectively adsorbed and desorbed oxygen.

References

1) a) J. P. Collman, *Acc. Chem. Res.*, **10**, 265 (1977); b) R. D. Jones, D. A. Summerville, and F. Basolo, *Chem. Rev.*, **79**, 139 (1979); c) E. Tsuchida and H. Nishide, *Top. Curr. Chem.*, **132**, 64 (1986).

2) J. P. Collman, R. R. Gagne, T. R. Halbert, and J. C. Marchon, *J. Am. Chem. Soc.*, **95**, 7868 (1973).

3) N. Toshima, "Polymers for Gas Separation," VCH Publishers, New York (1992).

4) E. Tsuchida, "Artificial Red Cells," John Wiley, New York (1995).

5) K. Eshima, Y. Yuasa, H. Nishide, and E. Tsuchida, *J. Chem. Soc., Chem. Commun.*, **1985**, 130.

6) E. Tsuchida, T. Komatsu, S. Kumamoto, K. Ando, and H. Nishide, *J. Chem. Soc., Perkin Trans. 2*, **1995**, 747.

7) J. P. Collman, R. R. Gagne, C. A. Reed, T. R. Halbert, G. Lang, and W. T. Robinson, *J. Am. Chem. Soc.*, **97**, 1427 (1975).

8) M. Calvin, R. H. Balies, and W. K. Wilmarth, *J. Am. Chem. Soc.*, **68**, 2254 (1946).

9) J. P. Collman, J. I. Brauman, K. M. Doxsee, T. R. Halbert, S. E. Hayes, and K. S. Suslick, *J. Am. Chem. Soc.*, **100**, 2761 (1978).

10) J. P. Collman, J. I. Brauman, K. M. Doxsee, T. R. Halbert, E. Bunnenberg, R. E. Linder, G. N. LaMar, J. D. Gaudio, G. Lang, and K. Spartalian, *J. Am. Chem. Soc.*, **102**, 4182 (1980).

11) D. K. White, J. B. Cannon, and T. G. Traylor, *J. Am. Chem. Soc.*, **101**, 2443 (1979).